25th ABCM International Congress of Mechanical Engineering
October 20-25, 2019, Uberlândia, MG, Brazil

COB-2019-1741
NUMERICAL METHODOLOGY FOR OBTAINING PERMEABILITY FOR 2D POROUS MEDIUM THROUGH FINITE VOLUME METHOD: a first-step towards more complex permeability functions

Pedro Matzembacher
Cirilo Seppi Bresolin
Guilherme Henrique Fiorot
Mechanical Engineering Department (DEMEC), Federal University of Rio Grande do Sul (UFRGS)
pmatzem@hotmail.com
cirilo.bresolin@ufrgs.br
guilherme.fiorot@ufrgs.br

Abstract. *The properties of porous medium are known to be very dependent on geometrical parameters. Many previous works from the literature employed experiments to propose correlations between those geometrical parameters and the permeability of the medium. Nowadays, the use of numerical simulation instead of experiments is a faster and less expensive alternative to obtain porous medium properties. In this work, numerical simulations employing finite volume schemes were performed to solve the flow of a non-Newtonian fluid through a 2D porous element. Flow properties were obtained and the Darcian flow was verified. Semi-empirical functions from the literature were tested against the numerical data found to the two-dimensional porous element simulated. The methodology here employed represent the first stage of a research that will aim for obtaining a more representative function for the permeability in non-Newtonian fluid flows.*

Keywords: *finite volumes method, non-Newtonian fluid, porous medium*

1. INTRODUCTION

Flows of the most different types of fluids, under various conditions (kinematic or dynamic), represent classic problems of the literature and are present in innumerable natural physical phenomena, as well as in several industrial processes. Flows of fluids that present non-Newtonian rheology are particularly noteworthy, as they exhibit hydrodynamic behavior and nonlinear relations between shear stress and strain rate. These fluids are present in several environments, for example:

- in the food industry, where those fluids are still combined with thermal phenomena which also affect their rheological properties;
- in the petroleum sector, for some drilling well methods, where the properties of drilling fluids must be versatile, being easily pumped and also capable of carrying the debris out;
- in many natural phenomena such as volcanic eruptions, debris and mud flows, snow avalanches, among many others, where the rheological properties affect their predictability.

Particularly, one can identify the flows that occur in the presence of porous surfaces or walls, which allow the fluid to flow through their voids. The presence of the porous medium affects the flow dynamics, changing the boundary condition of the flow, diverging from the classical adhesion condition to the sliding condition. This effect results in a non-zero velocity at the interface between the flow and the porous wall at rest. Such an effect can have important consequences such as increasing the average flow velocity (flow), decreasing the average height of a channel flow, among others. Scientific advances have been conducted in order to better understand what is happening in this interface.

An extensive review on experimental works was provided by Sochi (2010), where the authors explored the relation between pressure drop and porous media parameters for non-Newtonian fluids. In that work, the author explicitly mentioned that no unifying theory could show a clear relation between fluid and porous medium parameters. For each rheological constitutive law, a different function was found to express how the pressure drop was established, from power-law fluids (Sabiri and Comiti, 1995) to Herschel-Bulkley (Chevalier *et al.*, 2013). More recently, due to advances in experimental and computational technology, the study of flow past a cavity have been reaching new understandings about the slip velocity assumed by flow when crossing a porous element (Vigneaux *et al.*, 2018). Yet, no direct correlation of the cavity

parameters to the macroscopic porous medium behavior is observed. In that direction, a precise characterization of the macroscopic interface is still sought in the community, specially when it concerns a flow of the Herschel-Bulkley type that incorporates in a single rheological model the non-Newtonian effects of the yield stress and non-linearity between shear stress and strain rate.

The objective of this work is to developed a methodology to relate the permeability (or hydraulic conductivity) of porous media to non-Newtonian fluids presenting yield stress. In the first stage of this research brought in the present paper, numerical simulations employing Ansys/FLUENT software were performed to retrieve the classical relationships for Newtonian and power-law fluids crossing a 2D porous element with fixed geometrical properties. The results presented show that empirical relationships found in the literature cannot be directly employed as they were obtained for realistic 3D porous elements. Nevertheless, we show that many relationships from the literature can be employed to assess the validity of the models and experiments, and highlight the relation between Darcian-like flow across the pore element and its geometrical parameters. The next step in this research is to extrapolate such methodology to non-Newtonian fluids presenting yield stress and verify which geometrical parameters would relate to the macroscopic features of permeability.

2. METHODOLOGY

In this work, a classical two-dimensional Darcian flow was considered, where a non-Newtonian fluid with density ρ [kgm^{-3}] is pushed through a porous medium constituted by an assembling of rods with diameter d [m] and presenting a porosity ε. Isotherm flow is considered. A pressure gradient is developed in a preferable axis, and the flow assumes creeping motion at that same direction at constant velocity u_D. The flow is mainly dominated by the viscous forces, where the Reynolds number is always equal to the unity ($\mathrm{Re} = 1$).

The non-Newtonian fluid employed presented power-law rheology, which in simple shearing conditions can be represented by Eq. (1),

$$\tau = C\dot{\gamma}^n \tag{1}$$

where the the consistency C [Pas^n], and n is the flow index, which is responsible for the non-linearity between the shear stress τ and shear strain rate $\dot{\gamma}$. For $n = 1$, Eq. (1) represent a Newtonian fluid, and $C = \mu$ (dynamic viscosity).

In this conditions, the governing equation is summarized in Eq. (2) (Kaviany, 1991):

$$-\frac{\partial p}{\partial x} = \frac{\eta}{K} u_D; \tag{2}$$

where p is the pressure [Pa], x the longitudinal coordinate [m], η is the apparent viscosity [Pas] of the fluid,

$$\eta = \frac{\tau}{\dot{\gamma}} \tag{3}$$

and K is the permeability [m^2].

Given a well-controlled situation, the permeability function depends only on the geometry formed by the voids constituting the porous medium for a Newtonian fluid. However, for a power-law fluid, the flow index n also becomes important to asses the permeability, bringing an additional variable to the problem and increasing uncertainties. Many semi-empirical laws are available on the literature as, for example, Eq. (4), from Sahraoui and Kaviany (1992)

$$K_1 = 0.01515\pi d^2 \left(\frac{\varepsilon^{5.1}}{1-\varepsilon}\right) \tag{4}$$

for a Newtonian fluid, which presents good agreement for porosity between 0.40 and 0.80. For non-Newtonian fluids, the permeability becomes dependent of the flow index n, as shows Eq. (5) from Christopher and Middleman (1965) calibrated for $n > 0.70$,

$$K_n = \frac{6}{25}\left(\frac{n\varepsilon}{3n+1}\right)\left[\frac{\varepsilon d}{3(1-\varepsilon)}\right]^{n+1} \tag{5}$$

and Eq. (6) proposed by Sabiri and Comiti (1995),

$$K_n = \left(\frac{2n\varepsilon}{3n+1}\right)^n \left(\frac{d}{4T}\right)^{n+1} \tag{6}$$

where the subscript n identifies that the permeability is n-dependent, and T represents the tortuosity.

Based on these semi-empirical models, numerical simulations were performed to simulate a fluid flow past a two-dimensional porous element composed of circular solid shapes, equivalent to cylindrical rods perpendicular to the flow. Porous medium parameters were modified in order to evaluate their hydraulic conductivity to the fluid through velocity and pressure fields from numerical simulations. Semi-empirical models were then tested against the numerical results obtained.

2.1 Numerical simulation

The simulation were performed through the software Ansys/FLUENT (finite volume method) to solve the mass and momentum conservation equations. Isotherm conditions were forced, so energy conservation was not solved. Simulations were done for the steady case, considering pressure-velocity coupling. Second order schemes were used to obtain solution for the spatial derivatives (Tab. 1). Translational periodic boundary condition was employed for A and B contours, fixing the mass flow, while geometrical symmetry was employed for C and D contours (Fig. 1).

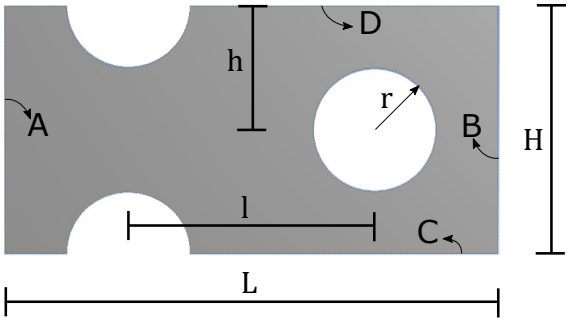

Figure 1. Domain employed for porous element simulations in Ansys/FLUENT.

Table 1. Detailing of the numerical schemes and meshing employed in the simulations.

Numerical Schemes		**Meshing Sizing**	
Spatial Discretization (Gradient)	Least Squares Cell Bases	Relevance Center	Fine
Spatial Discretization (Pressure)	Second Order	Smoothing	High
Spatial Discretization (Momentum)	Second Order Upwind	Min Size	5e-3
High Order Term Relaxation	0.10	Max Face Size	1e-2
		Max Size	1e-2

In order to ensure the precision and validity of all the simulations done in this work, a standard procedure of mesh generation was used for every case. Details are shown in Tab. 1. This method was used to guarantee and support the results convergence.

The velocity field $\vec{U}(x,y) = (u(x,y), v(x,y))$ and pressure gradients $\mathrm{d}p(x,y)/\,\mathrm{d}x$ results of each simulation were transferred to MATLAB for post-processing and obtaining of further data of the porous element.

2.2 Porous medium geometry

For a fixed radius r (diameter d) of arranged rods in the porous element, the porosity ε is calculated as the ratio of void area (where fluid can flow) to the total area of the 2D porous element. In this work, the geometrical properties of the porous medium were customized to obtain a target porosity ε. This customization, specified in Eq. (7), could allow the development of studies on the effect of the arrangement of the internal boundaries and size into the macroscopic function of the permeability.

$$\varepsilon = 1 - \frac{2\pi r^2}{HL} = 1 - \frac{2\pi r^2}{H(L/2 + 2r + 2l)} \tag{7}$$

where H and L are the vertical and horizontal lengths of the porous element, and h and l are the vertical and horizontal distances between rods, where $h = H/2$ and $l = L/2 - r$ in order to ensure the domain symmetry (Fig. 1). The set of

porosity values used to perform the simulations are presented in the Tab. 2, as well as the two principal dimension that characterize the domain.

Table 2. Set of porosity employed in the present study and geometrical properties.

Porous Element	ε	H	L
H1	0.70	4.00	5.24
V1	0.70	3.49	6.00
V2	0.60	3.00	5.24
V3	0.50	2.75	4.57
V4	0.40	2.30	4.53
V5	0.30	2.10	4.27

2.3 Test-fluid

Numerical simulations were performed employing a non-Newtonian fluid with power-law constitutive law, as shown in Eq. (1), where the the consistency C was fixed with a constant of 2.51 Pas^n for all the simulations. The flow index n varies from 0.30 to 1.00, so the results obtained characterized shear thinning fluids (for $n < 1$) and a Newtonian fluid (for $n = 1$). The density was fixed $\rho = 1000$ kgm^{-3}.

2.4 Reynolds number

In order to establish a relation between all simulations performed, the Reynolds number was maintained constant equals to the unity ($Re_n = 1$) for all simulations. An expression for the Reynolds number for power-law non-Newtonian fluids was used, as proposed by Madlener *et al.* (2009), in Eq. (8).

$$Re_n = \frac{\rho^{n-1} H^{2n-2} \dot{m}^{2-n}}{8^{n-1} C (\frac{3n+1}{4n})^n} \tag{8}$$

The mass flow $\dot{m}$ (expressed in terms of kgm^{-1}s^{-1}) at the boundaries A and B (Translational periodic boundaries) was adapted in each numerical run to respect the fixed Reynolds number condition based on Eq. (9).

$$\dot{m} = \left[\frac{8^{n-1} C \left(\frac{3n+1}{4n}\right)^n}{\rho^{n-1} H^{2n-2}} \right]^{\frac{1}{2-n}} \tag{9}$$

2.5 Permeability calculation

To obtain the value for the permeability through the numerical simulations K_0, we solved the Darcy equation (Eq. (10)),

$$\overline{\frac{\Delta p}{\Delta x}} = \frac{\eta}{K_0} u_D \tag{10}$$

where the pressure gradient was approximated by its numerical discrete difference, and the Darcian velocity u_D was computed as

$$u_D = \frac{\varepsilon}{T} u_P, \tag{11}$$

with T the numerically calculated tortuosity, u_P being the mean pore velocity calculated as mean velocity magnitude though the element

$$u_P = \overline{U(x,y)}, \tag{12}$$

and $U(x,y) = \sqrt{u(x,y)^2 + v(x,y)^2}$, where u and v are the x and y components of the velocity field.

Tortuosity is an important parameter that depends on the solid boundaries in the porous element arrangement and the flow regime. In order to save time and reduce the calculation complexity, the tortuosity was obtained by the method proposed by Matyka and Koza (2012), which consists in dividing the sum of the velocity magnitude for every position in the domain by the sum of the longitudinal velocity in the macroscopic flow direction component. This method is expressed mathematically by the Eq. (13)

$$T = \frac{\sum U(x,y)}{\sum u(x,y)} \tag{13}$$

For a Newtonian fluid ($n = 1$), the apparent viscosity is equal to the consistency parameter, so η is equivalent to the fluid dynamic viscosity, which is constant for the conditions here imposed. For a power-law fluid ($n \neq 1$), a special treatment for obtain the apparent viscosity is needed. The expression presented by Sabiri and Comiti (1995) to calculate the mean shear rate is employed, as presented in Eq. (14)

$$\dot{\gamma} = \left(\frac{3n+1}{2n}\right)\left(\frac{1-\varepsilon}{\varepsilon^2}\right) a_{vd} T u_P \tag{14}$$

where a_{vd} is the specific surface area of the porous medium defined as the ratio between the void surface and the total volume of the porous element. Finally, for a power-law fluid, the apparent viscosity is defined as

$$\eta = C\dot{\gamma}^{n-1} \tag{15}$$

For any test-fluid, the permeability K_0 of the porous element can then be calculated using Eq. (10).

3. RESULTS AND DISCUSSIONS

The numerical runs performed were first analyzed based on the domain (porous elements from Tab. 2). Permeability is plotted against the flow index n to show their relation on Fig. 2.

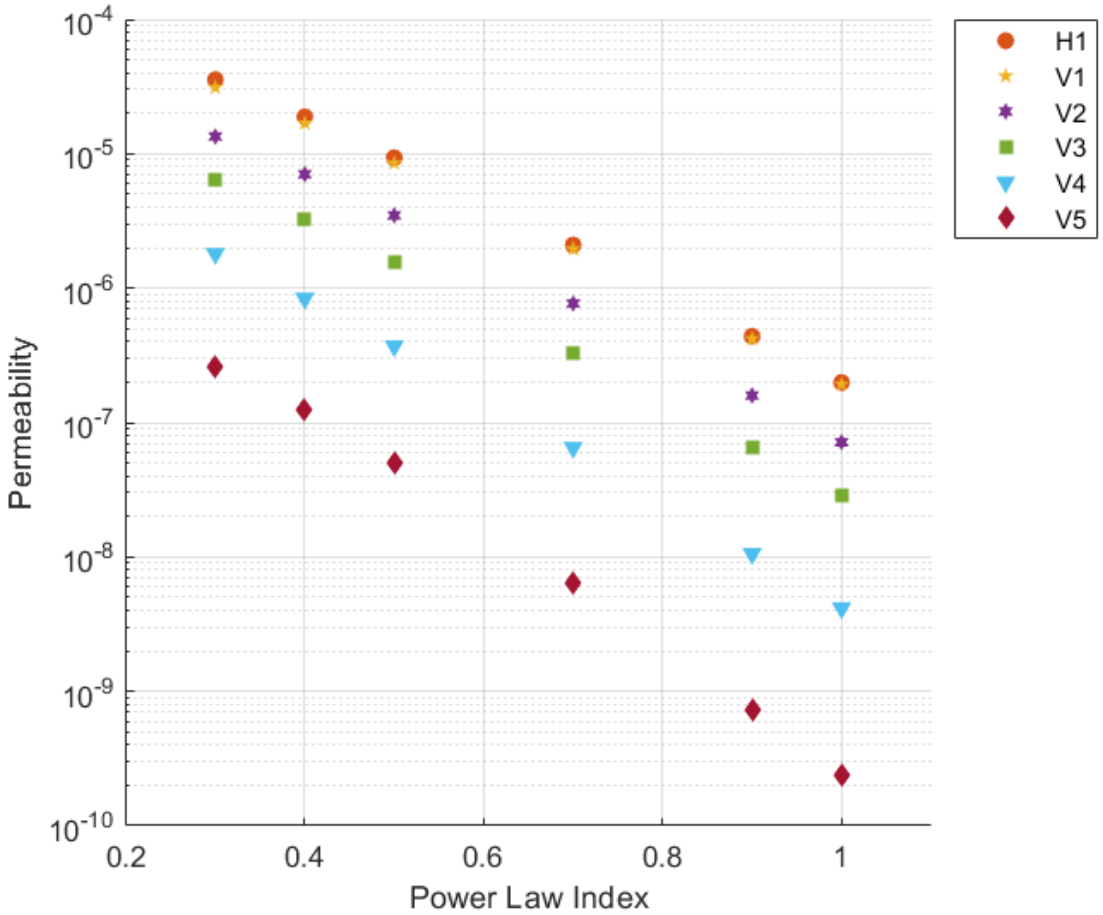

Figure 2. Numerical values for the permeability K_0 against the flow index n. Each symbol represents a porosity value and arrangement, following Tab. 2.

It can be seen that the permeability is affected by the non-Newtonian properties n, increasing as n decreases. This observation is in agreement with the physical behavior of a shear-thinning fluid: the stronger the non-Newtonian effect of n, fluid becomes less viscous for the same stress applied; in this way, for a fixed Re, flow velocity across the porous element increases, culminating in the effect observed. Also, as expected, for a decrease in the porosity. Another observation that can be done is that, for our test cases, the arrangement of particles did not contributed significantly to the permeability function as data from tests H1 and V1 suggests. This would be a matter for futures research since the range employed

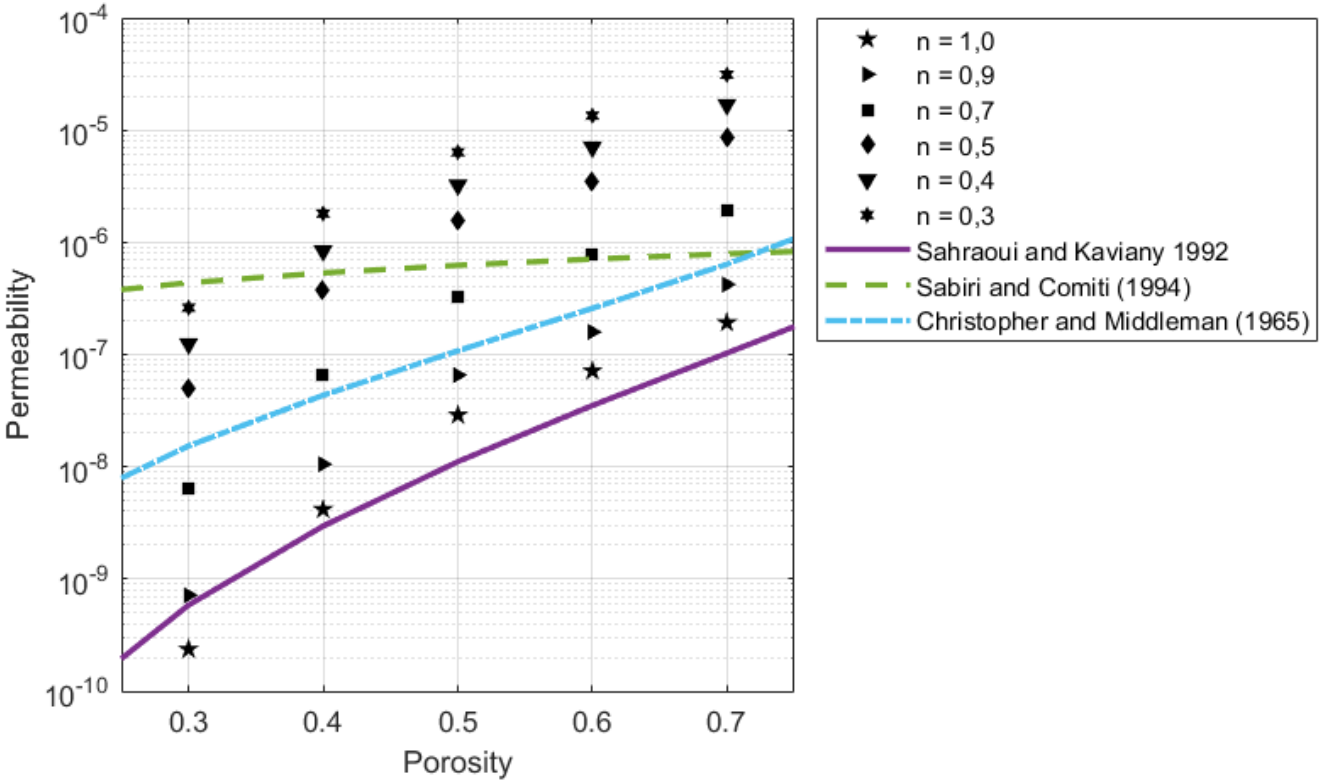

Figure 3. Numerical values for the permeability K_0 against the porosity ε, with permeability functions from the literature. Each symbol represents a porosity value and arrangement, following Tab. 2.

here for those tests was short.

Figure 3 presents another analyses on the data obtained, showing the numerically calculated permeability against the porosity ε. Those results are plotted together with three different semi-empirical relations expressed in Eq. (4), (5), and (6) for $n = 0.70$. The first observation that can be made is the behavior of the solution for the Newtonian fluid ($n = 1$) approximates classical formulations. The discrepancy observed could be a result of the tortuosity calculation that was performed in this methodology, and assumed/estimated in the previous work from Sahraoui and Kaviany (1992).

The numerical run represented by the square symbol (■) shows the test where $n = 0.70$. The comparison between the correlation proposed by Christopher and Middleman (1965) and the results obtained solving the Darcy equation show that the tendency of both curves are similar, showing a difference approximately less then one order of magnitude to the results obtained from the numerical run. They also follow the same pattern as the Newtonian case, as mentioned before. Nevertheless, the permeability obtained through the Darcy equation and numerical data has a faster growth than the semi-empirical function depending on the porosity. The differences between both methods for the permeability values could be explained by two main features: the expression from Eq. (5) was derived assuming a capillary model based on the Hagen-Poiseuille equation, while the simulations performed in the present work were based on the planar Hagen-Poiseuille; Christopher and Middleman (1965) did not take into count the medium tortuosity to establish their correlation, and when solving the Darcy equation, based on the numerical data, the tortuosity is used to evaluate the Darcyan velocity.

The results obtained from the correlation proposed by Sabiri and Comiti (1995) and the results obtained solving the Darcy equation are very different, presenting differences ins result that reaches almost 2 orders of magnitude for lower values of porosity. These discrepancies could be explained by 2 main reasons: the particle shapes used in the experiment are three dimensional objects, which is a feature that certainly present characteristics that are not represented by a simplified two-dimensional model; some experiments used particles that had high anisotropy, what increases the

experiment medium tortuosity and creates a big difference between the range of tortuosity used in the simulations and in the experiments. In the numerical runs performed, no anisotropy was explored.

4. CONCLUSION

This work presented a methodology for obtaining the permeability of a porous medium through numerical computation that could be tested for many different kinds of fluids. Through the results is possible to see that a direct correlation can be done through K_0 and K_n, and obtain a constant for proportionality/adjustment for the 2D porous element generated. It was also clear that the non-Newtonian effects interact with the porous medium geometry.

It was noticed that, for a preliminary test of medium arrangement (porous elements H1 and V1) with the same porosity, no clear effect of the solid bodies was observed, but this should be a matter of future research. The results of the simulations performed in each one of those two domains were compared to prove that the anisotropy flow properties, even existing, are so minor that could be neglected.

For the semi-empirical functions that were gathered for this work in comparisons with the numerical results, it was observed that their range of validity is intimately related to the experiments employed to calibrate them. In this way, a broader approach should be employed to better fit the relevant parameters to obtain a macroscopic function for the permeability, as function of the fluid and porous medium properties.

The next stage in this research is to perform numerical tests for non-Newtonian fluids presenting yield stress like a Bingham fluid, and also combining its effect with the non-linearity between shear stress and shear ratio, as Herschel-Bulkley fluids. These tasks will corroborate the results established in the literature and also shed light on the different friction laws offered by pore network to fluids of complex rheology.

5. ACKNOWLEDGEMENTS

The authors would like to thank PROPESQ-UFRGS for the administrative and financial support in this research.

6. REFERENCES

Chevalier, T., Chevalier, C., Clain, X., Dupla, J., Canou, J., Rodts, S. and Coussot, P., 2013. "Darcy's law for yield stress fluid flowing through a porous medium". *Journal of Non-Newtonian Fluid Mechanics*, Vol. 195, pp. 57–66.

Christopher, R.H. and Middleman, S., 1965. "Power-law flow through a packed tube". *Industrial and Engineering Chemistry Fundamentals*, Vol. 4, No. 4, pp. 422–426. ISSN 01964313. doi:10.1021/i160016a011.

Kaviany, M., 1991. *Principles of heat transfer in porous media*. Springer-Verlag New York. ISBN 3540975934 0387975934.

Madlener, K., Frey, B. and Ciezki, H.K., 2009. "Generalized Reynolds number for non-Newtonian fluids". *Progress in Propulsion Physics*, Vol. 1, pp. 237–250. doi:10.1051/eucass/200901237.

Matyka, M. and Koza, Z., 2012. "How to calculate tortuosity easily?" *AIP Conference Proceedings*, Vol. 1453, No. 1, pp. 17–22. doi:10.1063/1.4711147. URL `https://aip.scitation.org/doi/abs/10.1063/1.4711147`.

Sabiri, N.E. and Comiti, J., 1995. "Pressure drop in non-Newtonian purely viscous fluid flow through porous media". *Chemical Engineering Science*, Vol. 50, No. 7, pp. 1193–1201.

Sahraoui, M. and Kaviany, M., 1992. "Slip and no-slip velocity boundary conditions at interface of porous, plain media". *International Journal of Heat and Mass Transfer*, Vol. 35, No. 4, pp. 1–24.

Sochi, T., 2010. "Flow of non-newtonian fluids in porous media". *Journal of Polymer Science Part B: Polymer Physics*, Vol. 48, No. 23, pp. 2437–2767. ISSN 08876266. doi:10.1002/polb.22144.

Vigneaux, P., Chambon, G., Marly, A., Luu, L.h. and Philippe, P., 2018. "Flow of a yield-stress fluid over a cavity : Experimental and numerical investigation of a viscoplastic boundary layer". *Journal of Non-Newtonian Fluid Mechanics*, Vol. 261, No. August, pp. 38–49. ISSN 0377-0257. doi:10.1016/j.jnnfm.2018.08.005.

7. RESPONSIBILITY NOTICE

The authors are the only responsible for the printed material included in this paper.